Available online at www.sciencedirect.com
SCIENCE DIRECT
Coastal Engineering 53 (2006) 191 – 208
Coastal Engineering
An International Journal for Coastal, Harbour and Offshore Engineers
www.elsevier.com/locate/coastaleng

Rip current review

Jamie H. MacMahan [a,*], Ed B. Thornton [b], Ad J.H.M. Reniers [c]

[a] Center for Applied Coastal Research, University of Delaware, Newark, DE 19716, USA
[b] Oceanography Department, Naval Postgraduate School, Monterey, CA, 93943, USA
[c] Civil Engineering and Geosciences, Delft University of Technology, Delft, The Netherlands

Available online 1 December 2005

Abstract

Rip currents are shore-normal, narrow, seaward-flowing currents that originate within surf zone, extend seaward of the breaking region (rip head), and can obtain relatively high velocities. Within the last decade, there have been a significant number of laboratory and field observations within rip current systems. An overview of rip current kinematics based on these observations and the scientific advances obtained from these efforts are synthesized. Rip current flows are partitioned into mean, infragravity, very low frequency (vorticity), and tidal contributions, and it is found that each contributes significantly to the total. Data from the laboratory and the field suggest that the rip current strength increases with increasing wave energy and decreasing water depths. The maximum mean current occurs inside the surf zone, where the maximum forcing is present owing to the dissipation of waves.

Keywords: Rip currents; Morphodynamics; Nearshore; Hydrodynamics

1. The formation of a rip current

Rip currents are approximately shore-normal, seaward-directed jets that originate within the surf zone and broaden outside the breaking region (Figs. 1 and 2). There are weaker and broader onshore directed flows in the region neighboring the rip current, contributing to the alongshore directed feeder currents that converge to the rip current (Figs. 1 and 2). Early studies obtained crude estimates of rip current velocities, which include 0–2 Knots (0–1 m/s) (Shepard and Inman, 1950), 50 cm/s (Sonu, 1972), 30 cm/s (Huntley et al., 1988), and 70 cm/s (Short and Hogan, 1994). Mega-rips are generally observed on embayed beaches with suggested velocities exceeding 2 m/s (Short, 1999), but there are no in situ field measurements of mega-rips. Rip currents shape the sandy shoreline and may be important for transporting sediments offshore (Cooke, 1970; Komar, 1971; Short, 1999). Rip currents account for more than 80% of lifeguard rescue efforts, and are the number one natural hazard in the state of Florida. More people fall victim to rip currents in Florida, than to lighting, hurricanes, and tornadoes (Luschine, 1991; Lascody, 1998).

1.1. Theory of rip currents

The first attempt to explain rip currents was based on the kinematic argument that the onshore mass transport by waves over an alongshore bar most efficiently exits through a rip channel to form a rip current (Munk, 1949a,b) and more recently by Aagaard et al. (1997) and Brander and Short (2001). Although obviously mass must be conserved, Kennedy and Thomas (2004) argue that as the spacing between rip currents extends to infinity, the flow through the rip channel would also have to tend to infinity, which obviously does not happen. Svendsen et al. (2000) numerically found that the total transport through the rip channel does not depend on the spacing of the rip channels, and preliminary analysis from the Nearshore Canyon Experiment (NCEX) supports this (MacMahan et al., submitted for publication).

All dynamical models of rip currents are forced by alongshore variations of wave height that result in alongshore variations in wave-induced momentum flux, termed radiation stress by Longuet-Higgins and Stewart (1964). A convenient starting point is the depth-integrated, horizontal

* Corresponding author.
E-mail addresses: macmahan@coastal.udel.edu (J.H. MacMahan), thornton@nps.edu (E.B. Thornton), ad@dutcvmm.ct.tudelft.nl (A.J.H.M. Reniers).

0378-3839/$ - see front matter © 2005 Elsevier B.V. All rights reserved.
doi:10.1016/j.coastaleng.2005.10.009

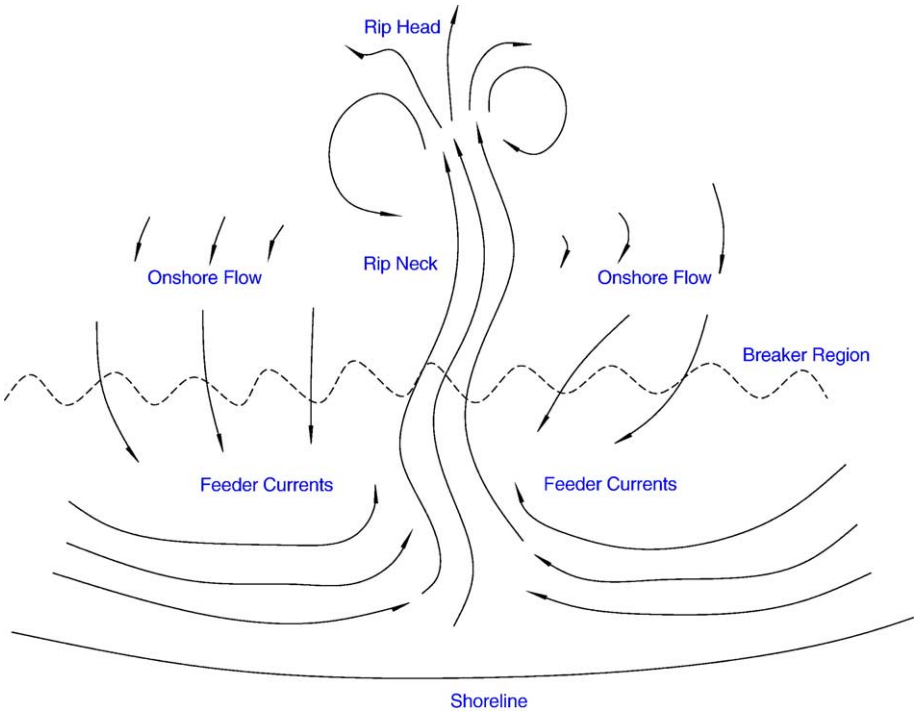

Fig. 1. A schematic of a rip current similar to the classical definition by Shepard et al. (1941).

momentum balance equations that are averaged over many wave groups representing stationary wave conditions (see Phillips, 1977)

$$\frac{d}{dx_j}\left(\tilde{U}_i\tilde{M}_j + S_{ij}\right) = -\rho g(h+\bar{\eta})\frac{d\bar{\eta}}{dx_i} + R_i, \tag{1}$$

where $i,j=1,2$, and $\tilde{M}_j$ is the total mean momentum flux per unit area, $\tilde{U}_i$ is the depth averaged velocity $\left(\tilde{U}_i = \frac{\tilde{M}_i}{\rho(h+\bar{\eta})}\right)$, S_{ij} are the radiation stresses, η is the mean water level and h the still water depth, and R_i are the stresses. Considering the cross-shore (x) momentum balance equation, and assuming the waves are normally incident and bottom contours straight and parallel, changes in cross-shore radiation stress, S_{xx}, are balanced by the hydrostatic pressure gradient,

$$\frac{dS_{xx}}{dx} = -\rho g(h+\bar{\eta})\frac{d\bar{\eta}}{dx}, \tag{2}$$

where ρ is the density of seawater and g is the gravitational acceleration. Applying linear wave theory in shallow water, $S_{xx}=(3/2)E$, where E is wave energy, results in wave set-down outside the surf zone as the wave energy increases due to shoaling, and set-up inside the surf zone as the waves break and the energy decreases (see for example Bowen, 1969). The vertical imbalance between the cross-shore pressure gradient and wave forcing produces an offshore

Fig. 2. A snap shot of a rip current in Monterey Bay, CA. The rip current is the dark patch. There is intense wave breaking on both sides of the rip currents with little breaking within the deeper rip channel, where bubbles are advected seaward.

return flow within the surfzone between the bed and the trough (Dyhr-Nielsen and Sorensen, 1970) that often is referred to as undertow.

In the three-dimensional case of alongshore variations in wave height of normally incident waves on an alongshore uniform beach, the larger waves generate larger set-down/up, which creates alongshore pressure gradients both outside and inside the surf zone. Considering the alongshore (y) momentum equation, forcing is given by

$$Fy = -\frac{dS_{yy}}{dy} - \rho g(h+\bar{\eta})\frac{d\bar{\eta}}{dy}, \quad (3)$$

where $S_{yy}=E/2$ in shallow water. Outside the surf zone the alongshore pressure gradient is balanced by the alongshore gradient in radiation stress. However, inside the surf zone, the gradients in the alongshore radiation stress and pressure act together to produce a flow of water from the regions of high waves to the regions of low waves. Approximating wave breaking as proportional to the total depth of water $H=\gamma(h+\eta)$, and $E=1/8\rho g H^2$, the alongshore momentum balance in the surfzone is given by:

$$Fy = -\frac{1}{8}\rho g\gamma^2(h+\bar{\eta})\frac{d(h+\bar{\eta})}{dy} - \rho g(h+\bar{\eta})\frac{d\bar{\eta}}{dy}. \quad (4)$$

Now considering the case of a nominally 1m deep rip channel incised into a low tide terrace bar at 200 m intervals, i.e., $\frac{\delta h}{\delta y} = O(0.01)$. Owing to the combined bottom and rip-current refraction the shear component of the radiation stress, $\frac{\delta S_{xy}}{\delta x}$, is assumed to be small relative to the other terms considered here (Haller et al., 2002). In that case, the alongshore radiation stress forcing term is of the same magnitude and direction as the alongshore pressure gradient. The result is convergence of longshore currents within the surf zone to the region of low waves, where the flow exits the surf zone as a confined rip current (Fig. 1). This was first explained by Bowen (1969) and illuminated by Battjes (1988).

An alternative approach in examining the dynamics is to use the vorticity equation, which is obtained by cross-differentiating the horizontal momentum equations to eliminate the pressure gradients in horizontal directions. Here the circulation is maintained by the torque that is generated by the radiation stress gradients, particularly in the alongshore direction inside the surf zone (Bowen, 1969; Oh and Dean, 1996). Arthur (1962), considering only the nonlinear terms in the vorticity equation, argued that in the absence of friction, the potential vorticity is conserved along a stream line. As the rip current moves offshore into deeper water, the streamlines move closer together creating a stronger and narrower current, which explains why even when a rip channel occurs over a gentle alongshore depression, the offshore jet is well confined. This approach is conceptually elaborated upon by Peregrine (1998) and Kennedy and Thomas (2004).

Rip spacing is often observed to be quasi-periodic at O(100 m), motivating modelling efforts to find and impose alongshore perturbations on this scale. Mechanisms used to explain alongshore variations in wave height can either be wave–wave interactions (such as edge waves and incident waves (Bowen and Inman, 1969)), or imposed perturbations either on wave height directly, or on bathymetry, that results in variations in wave height owing to shoaling, refraction and breaking (Dalrymple, 1975).

Starting with models on alongshore homogeneous beaches, Dalrymple and Lozano (1978) imposed alongshore wave height variations to show that refraction by the outgoing rip current causes the waves to impinge on the beach obliquely, generating convergent longshore currents, which then flow offshore as a rip current. The result is a self-sustaining rip current, although the initial perturbation on the wave heights is not addressed. Alongshore variations of wave height can also be the result of wave–wave interactions. Bowen and Inman (1969) demonstrated that incident wave interactions with synchronous standing edge waves can lead to alongshore variation of incident waves at the scale of the edge waves. However, the edge wave spacing is generally too short for observations of rip current spacing. Symonds and Ranasinghe (2000) considered the interaction of wave groups and edge waves, which provides a much longer spacing, more in line with field observations. Fowler and Dalrymple (1990) and Fowler (1991) showed that wave groups composed of two wave trains at slightly different frequencies and incident at angles, θ, from opposing quadrants result in a spatially varying wave energy pattern, where the alongshore length scale is determined by the alongshore wave number difference between the two wave trains, $\Delta k_y = k_1\sin\theta_1 - k_2\sin\theta_2$, and the timescale is determined by their difference frequency, $\Delta f = f_1 - f_2$. When the waves break, the changes in radiation stresses generate slowly migrating rip currents traveling alongshore at $C = \frac{\Delta f}{\Delta k_y}$. For the special case of the wave trains having the same frequency, the circulation pattern is stationary (Dalrymple, 1975). The alongshore length scale of the Δk_y can be comparable to observed rip current spacing.

Ryrie (1983) considered a single wave group with limited, sharp peaked, alongshore dimension. The resulting variations in radiation stresses generate both transients and a steady circulation cell, which is left behind after the wave group has dissipated due to wave breaking and the transient motions dispersed. The circulation has a very low frequency signal as it is slowly dissipated by friction. A wave group in nature is not sharp peaked, but typically varies smoothly, which results in the generation of two circulation cells of opposite vorticity (Peregrine, 1998; Buhler and Jacobson, 2001).

Reniers et al. (2004) generalized the hydrodynamic response to wave group forcing by considering the evolution of temporally and spatially varying wave group energy owing to an incident directional short-wave spectrum forcing low frequency motions. The model resolves the time dependence of the wave group energy, which appears as random “blobs” of energy (Fig. 3), representing the stochastic nature of wave groups. When adjacent pairs of wave groups offset in time and space enter the surf zone, the interaction of the generated vortices can lead to narrow, offshore-directed, quasi steady flows. Over an alongshore homogeneous bathymetry, the

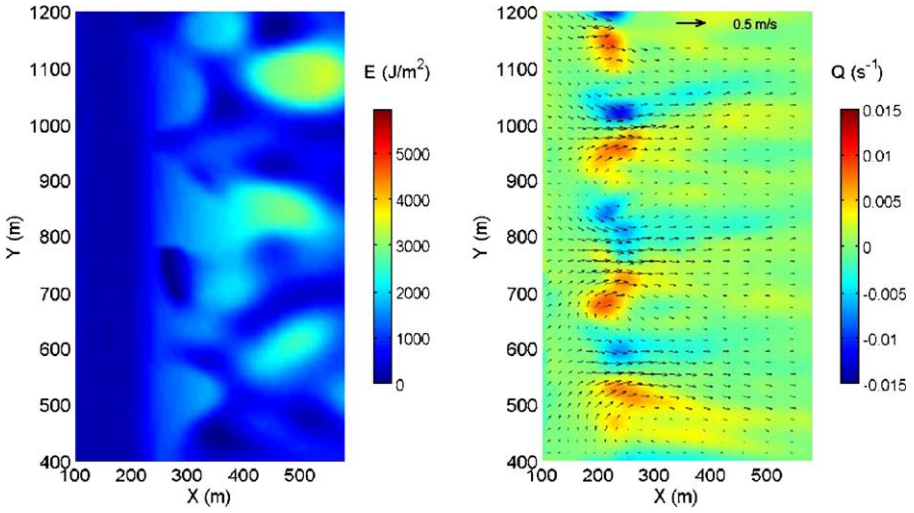

Fig. 3. Left panel: Snap shots of spatially modulated wave group energy incident on a single-barred, alongshore uniform beach (shoreline at left). Right panel: Snap shot of corresponding very low frequency, f<0.004 Hz, velocity and vorticity field.

circulation cells, in general, propagate slowly alongshore, simulating migrating rip currents.

Rip currents are most often observed to occur when the waves approach at near normal incidence and where there are alongshore variations in bathymetry with the alongshore sand bar incised by rip channels. Bowen (1969) was the first to show that alongshore perturbations in bathymetry result in alongshore variations in wave height, which generate rip currents. A number of models have followed with various refinements, which include improved nonlinear bottom shear stress and turbulent momentum mixing (e.g., Noda, 1974; Dalrymple et al., 1977; Mei and Liu, 1977; Ebersole and Dalrymple, 1980; Wu and Liu, 1985, and others). More recent models, although forced by monochromatic waves, allow for time dependence, include nonlinear Boussinesq waves in which wave–current interaction is incorporated (Sorensen et al., 1998; Chen et al., 1999), and have a quasi-3D formulation (Haas et al., 2003). Wave–current interaction is included by Yu and Slinn (2003), who find that the rip current produces a negative feedback on the wave forcing to reduce the strength and offshore extent of the flow. Complex flow patterns result with instabilities formed at the feeder currents with the unsteady rip flow characterized by vortex shedding.

1.2. Morphodynamics

Morphodynamic models attempt to answer why the quasi-periodic alongshore perturbations in the bathymetry, usually identified as rip channels, occur at the observed alongshore spacing O(100 m). Morphodynamic models can be categorized as forced or free (also referred to as (in)stability, Dodd et al. (2003) or self-organized Blondeaux (2001). Only models that incorporate normally incident mean wave direction, conducive to the development and maintenance of rip currents, are considered here. In forced process models, the three-dimensional pattern of the hydrodynamics imposes a similar pattern on the morphology (sometimes referred to as a template model (Holman, 2000)), and there is no feedback between the morphology and the hydrodynamics. Edge waves with comparable alongshore length scales to observed rip channel spacing have been used to force these models (Bowen and Inman, 1969; Holman and Bowen, 1982). The edge wave models require energy focused at a single dominant frequency. However, measurements show that edge waves are generally broad-banded without a dominant frequency (see e.g., Sallenger and Holman, 1987).

Morphodynamic stability models were reviewed by Dodd et al. (2003) and discussed in particular in relation to crescentic bars by Van Enckevort et al. (2004). These models allow for a positive feedback between the hydrodynamics and the sediment transport forming the morphology, in which the morphodynamic response does not mirror the hydrodynamic forcing.

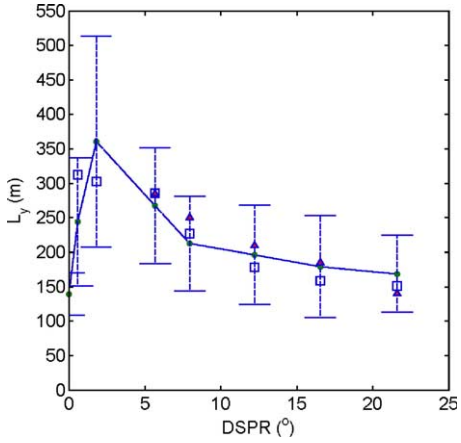

Fig. 4. Model predicted average alongshore spacing between rip channels (dots) as a function of directional spreading (DSPR) for one-meter wave height with mean wave direction normal to shore. The bars indicate the standard deviation of an ensemble of 8 simulations. Corresponding alongshore length scales of incident wave groups (triangles) and quasi-steady circulations (squares). Reproduced from Reniers et al. (2004) with permission from the American Geophysical Union.

The hydrodynamics are generally described by simplified depth-integrated conservation equations for mass and momentum, with sediment transport and morphology components. Starting from an alongshore-uniform equilibrium profile state, the time development of periodic perturbations superimposed on the morphology at varying alongshore length scale is examined. The problem is linearized by assuming small perturbations. If there is a positive feedback, the perturbation on the morphology can grow. The growth rate rates are solved for various alongshore length scales of the perturbation, and it is assumed the wave-length associated with the fastest growing mode corresponds to the rip channel spacing. Since a single mode is obtained, the resulting morphology is necessarily periodic, and since the problem is limited to small perturbations, only the initial growth of the perturbations can be examined. Hino (1974) was the first to utilize linear stability analysis and found that the alongshore scale of the rip channels was approximately four times the width of the bar crest to shoreline. This earlier work was revisited by Falques et al. (2000) for waves normally incident on an initially planar beach and by Deigaard et al. (1999) for an initially alongshore uniform barred-beach. The rip spacing is found to be related to the surf zone width.

Nonlinear stability analysis allows finite perturbations, and the final amplitude of the perturbations can be solved. Nonlinear solutions may contain multiple modes such that the resulting spacing is quasi-periodic resembling nature. Damgaard et al. (2002) employed a nonlinear hydrodynamical flow model coupled to sediment transport and morphology forced by normally incident monochromatic waves with a stochastic perturbation on bathymetry, and found that the rip channel spacing did not depend on wave height, but did depend of the width of the bar crest to shoreline as found earlier by Hino (1974) and Deigaard et al. (1999).

Table 1
Field observations of rip currents

Location	Reference	Instrumentation	Duration	Survey tech.	Offshore wave observation
LaJolla, CA	Shepard, 1936; Shepard et al., 1941; Shepard and Inman, 1950	Visual observations, wave machine, tidal elevation, tsunami recorders, drifters, pressure sensors	8 total days	Swimmer height and wire sounding	Pressure
LaJolla, CA; Torrey Pines, CA	Inman and Quinn, 1952	Visual observations, drifters	35 total days	Not available	Visual
New South Wales, AU	McKenzie, 1958	Visual	Months	Visual	None
Sea Grove, FL	Sonu, 1972	Neutrally buoyant drifter balls, bi-directional ducted current meters, resistance wires, tethered camera balloon and dye, stilling wells	3 days	Rod and level (swimmer)	None
Ajigura Beach, Japan	Sasaki and Horikawa, 1975, 1978	Video and floats	4 days	Soundings	Directional
Herzliya Beach, Israel	Bowman et al., 1988a,b	2 bidirectional ems	16 total days	Rod and level (swimmer)	Waverider (33 km away)
Kingston, Jamaica	Huntley et al., 1988	Dye tracking	3 day	Rod and level (swimmer)	Pressure
LaJolla, CA	Smith and Largier, 1995	Phase-Doppler array, CTDw/OBS	5 days	None	Pressure
Skallingen, Denmark	Aagaard et al., 1997	6 bi-directional current meters, 9 optical backscatter sensors, 1 pressure sensor	14 days	Rod and level echosounder	Pressure
Palm Beach, AU	Brander, 1999; Brander and Short, 2001	5 co-located duct-current meters and pressure sensors, dye	7 days, 3 days	Total station	None
Muriwai Beach, NZL	Brander and Short, 2000	3 co-located duct-current meters and pressure sensors, Lagrangian measurements of swimmers	2 days	Total station	None
LaJolla, CA	Vagle et al., 2001	Horizontal Doppler sonars	7 days	None	Pressure
Monterey, CA	MacMahan et al., 2004a,b, 2005	Arrays of electromagnetic current meters, pressure sensors, ADCP	44 days	Personal watercraft	Directional wave buoy
Moreton Island, AU	Callaghan et al., 2004	3 ADCPs, stilling wells	3 days	Rod and level	None
LaJolla, CA	Schmidt et al., 2003, in press	GPS drifters	2 days	Personal watercraft	Pressure
Torrey Pines, CA	MacMahan et al., submitted for publication	Arrays of electromagnetic current meters, pressure sensors, ADCP	20 days	Personal watercraft	Directional ADCP

All previous dynamic and morphodynamic rip current models employed monochromatic waves. Reniers et al. (2004) coupled their nonlinear, shallow water, flow model to sediment transport and morphology components, and forced the model by wave groups obtained from a directional spectrum with a mean wave angle normal to shore. The wave groups generate gradients in radiation stress and pressure that force low frequency vortices (Fig. 3). The low frequency vortices perturb the initially alongshore uniform barred beach at the length scale of the groups. The vortices become coupled to the morphology as perturbations grow into rip channels owing to a positive feedback by the morphology on the hydrodynamics. The resulting rip channel spacing is random, but with a mean alongshore length scale similar to observations and at the same mean alongshore length scale of the wave groups (Fig. 4). The alongshore length scale of the wave groups is shown to be proportional to the directional spreading of the short waves and is related to the wave energy. Interestingly, infragravity waves (including edge waves) had little affect on the morphology except to smooth the bathymetry. Owing to the nonlinearities and broadband forcing of the model, the model appears to possess the characteristics of both forcing and self-organization.

In summary, all morphodynamic models, whether linear or nonlinear stability models, or nonlinear morphodynamic models forced by monochromatic waves or a directional spectrum, give rip channel spacing that is $O(100\ \mathrm{m})$ as observed in nature. Thus, it is difficult to discriminate the generation mechanism for rip channels.

2. Rip current observations

Most field observations of rip currents have been coupled to the underlying beach morphology (Shepard et al., 1941; Aagaard et al., 1997; Short, 1999; Brander and Short, 2001; MacMahan et al., 2005; amongst others). Rip current morphology generally consists of a feeder channel that is parallel to the shoreline, which converges to a deeper rip channel that is oriented in an approximate shore-normal direction. The rip channel can be an incised channel within a shore-connected shoal (transverse bar) or cuts through an alongshore bar. There have been attempts to measure the alongshore pressure gradients within the field using different stilling well designs (Sonu, 1972; Nielsen et al., 2001; Callaghan et al., 2004). These efforts have so far eluded a clear and accurate conclusion.

Within the last decade, there have been an increasing number of field experiments involving rip currents, which has lead to advances in our understanding of these systems. There have been 7 experiments (Seagrove, FL; Monterey, CA; LaJolla, CA; Torrey Pines, CA) in the USA (Sonu, 1972; Smith and Largier, 1995; Schmidt et al., in press; MacMahan et al., 2005, submitted for publication), 1 experiment in Denmark (Aagaard et al., 1997), 3 in Australia (Gold Coast, Moreton Island, and Palm Beach) (Brander and Short, 2000; Johnson and Pattiaratchi, 2004; Callaghan et al., 2004), 1 in New Zealand (Muriwai) (Brander, 1999), and 1 in Israel (Bowman et al., 1988a,b). The field observations varied from a few fortuitously located instruments to comprehensive efforts to instrument a rip current system. A summary of the rip current field attempts is outlined in Table 1. Durations of rip current experiments have ranged from hours to several weeks.

Table 2
Field results of rip currents

Location	Reference	Results
LaJolla, CA	Shepard, 1936; Shepard et al., 1941; Shepard and Inman, 1950	Classical description, visual identification, bathymetric and shoreline relations, qualitative tidal and wave influences, qualitative ripcurrent pulsations
LaJolla, CA; Torrey Pines, CA	Inman and Quinn, 1952	Qualitative vertical and horizontal flow structure by drogues
New South Wales, AU	McKenzie, 1958	Qualitative assessment of rip current spacing versus wave energy
Sea Grove, FL	Sonu, 1972	Flow characteristics, attempt to measure pressure gradients, vertical flow structure, suggested surf beat rip current pulsations, discussed tidal effects
Ajigura Beach, Japan	Sasaki and Horikawa, 1975, 1978	Flow observations
Herzliya Beach, Israel	Bowman et al., 1988a,b	Observations of rip current flow direction, pulsations, sediment patterns
Kingston, Jamaica	Huntley et al., 1988	Qualitative description of rip flow pattern
LaJolla, CA	Smith and Largier, 1995	Quantitative measurements of episodic pulsations and vortex movement outside the breaker region
Skallingen, Denmark	Aagaard et al., 1997	Sediment flux estimates, tidal modulation, mass transport conceptual model
Palm Beach, AU	Brander, 1999; Brander and Short, 2001	Tidal modulations, morphodynamic descriptions, sediment flux, very low frequency motions, wave parameter and mass transport conceptual model
Muriwai Beach, NZL	Brander and Short, 2000	Observations of tidal modulation and morphodynamics
LaJolla, CA	Vagle et al., 2001	Distribution and advection of bubbles in a rip current system
Monterey, CA	MacMahan et al., 2004a,b, 2005	Theoretical validation of infragravity rip current pulsations, conceptual model of rip current VLFs, tidal modulation, dimensionless relationships, morphodynamics
Moreton Island, AU	Callaghan et al., 2004	Pressure gradient, modulations of rip current
LaJolla, CA	Schmidt et al., 2003	Observations of bathymetrically-influenced rip current eddy
Torrey Pines, CA	MacMahan et al., 2005, submitted for publication	Cross- and alongshore distribution of waves and currents for a weak rip current

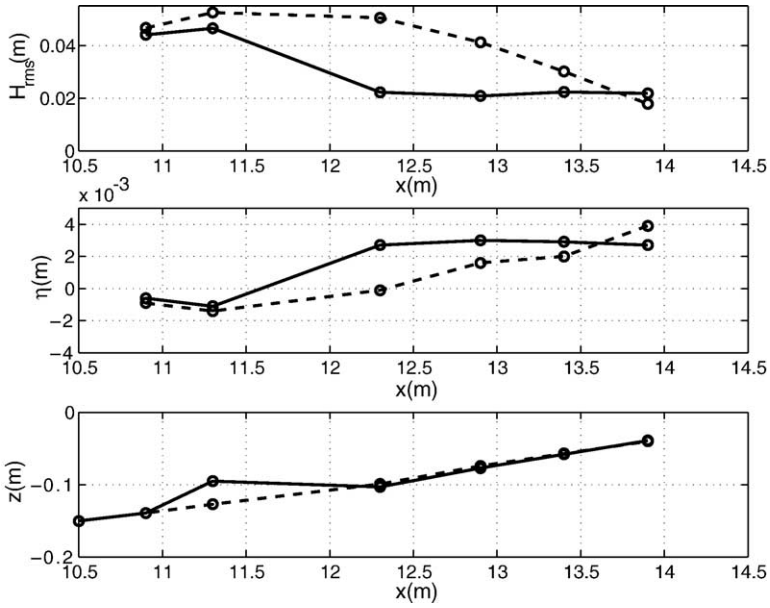

Fig. 5. Cross shore profiles across the bar (solid lines) and through the rip channel (dashed lines) of a) H_{rms} b) $\bar{\eta}$, and c) depth. Reproduced from Haller et al. (1997) with permission from the American Society of Civil Engineers.

Complete rip current experiments require three types of measurements, assuming the conditions exist for the generation of rip currents; 1) comprehensive velocity measurements within the rip channel and neighboring shoal, 2) accurate measure of the bathymetry, and 3) offshore directional wave measurements. Considerable difficulties are encountered in simultaneously obtaining all three of these measurements and, as a consequence, our understanding of rip currents has developed in a piecewise manner (Table 2). A chronological outline of results is presented in Table 2. Early qualitative observations suggested that the rip currents were coupled to the morphology, the rip currents pulsated, and the velocities increased with increasing wave height (Shepard, 1936; Shepard et al., 1941; Shepard and Inman, 1950; McKenzie, 1958; Bowman et al., 1988a,b). Recent studies have increased both spatial and temporal resolution of the observations and with greater accuracies, which have quantified earlier qualitative assessments. In addition, observations have been theoretically defined in greater detail.

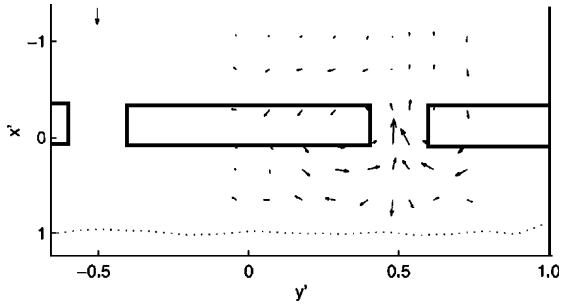

Fig. 6. Depth-averaged velocities from the same laboratory setting as in Fig. 5. Vector at upper left represents 10 cm/s; MWL at the shoreline is shown as a dotted line. Reproduced from Haller et al. (2002) with permission from the American Geophysical Union.

In addition to the field observations, there have been a number of recent laboratory experiments that have been used for theoretical verification and for interpretation of field measurements (Hamm, 1992; Oh and Dean, 1996; Haller et al., 1997; Dronen et al., 2002; Haller and Dalrymple, 2001; Haller et al., 2002; Haas and Svendsen, 2002; Kennedy and Thomas, 2004). Most field observations of rip currents are associated with incised rip channels in shore-connected shoals or depressions on near-planar beaches, while, with the exception of Hamm (1992), all laboratory measurements have been with an alongshore bar-trough beach cut by a rip channel.

A comprehensive description of rip currents was obtained in the laboratory with a longshore bar-trough beach incised by rip channels (lower panel, Fig. 5) (Haller et al., 2002). Waves are dissipated over the bar, while the waves in the rip channel are larger owing to wave–current interaction, and dissipated closer to shore (upper panel, Fig. 5). Wave set-up over the bar profile is larger than within the rip channel (middle panel, Fig. 5), and the resulting pressure gradients drive currents alongshore that converge to the region of lower set-up (the rip channel) generating a rip current (Fig. 6).

The combined results for field and laboratory measurements are described in the following.

3. Rip current flow

Rip current flows are forced by the incoming wave energy, and influenced by tidal elevation and the shape of the morphology. Hourly mean flows for various beaches have been tabulated (Table 3). The mean velocities are often small, yet the maximum values can be large. For example, the mean rip current velocities were $O(0.3)$ m/s during RIPEX (RIP current EXperiment) for a wide range of wave conditions, with maximum hourly mean rip current velocities approaching

Table 3
Field characteristics of rip currents (* estimated to MSL), where U_r is the rip current cross-shore velocity, U_{max} is the maximum documented rip current velocity, λ_r is the rip channel spacing, w_r is the rip channel width, h_r^* is the rip channel depth, h_b^* is the bar height, H_{mo} is significant wave height, T_p is the peak wave period, and D_{50} is the median sediment size

Location	U_r (m/s)	U_{max} (m/s)	λ_r (m)	w_r (m)	h_r^* (m)	h_b^* (m)	H_{mo} (m)	T_p (s)	D_{50} (mm)
Skallingen, NED	0.3	1.7	90	150	1.25	1	0.8	8	0.25
Palm Beach, AUS	0.4	2	200	60	1.8	1	0.75	10	0.35
Muriwai, NZL	0.65	2	500	150	1.5	1	1.5	14	0.25
Moreton Island, AUS	0.4	1	300	35	1.4	1	0.5	10	0.2
Torrey Pines, CA, USA	0.2	1	300	100	1.25	1	0.5	12	0.1
Monterey, CA, USA	0.3	2	125	60	1.5	1	1.5	12	0.35
SeaGrove, FL, USA	0.35	1.25	60	30	0.8	0.3	0.5	8	0.3

1 m/s, during an extreme storm, $H_{mo}>3$ m. Yet the one-minute averaged velocities approach 2 m/s. The variation in water level owing to the tide can also vary the flow velocity significantly over the course of a few hours (Shepard and Inman, 1950; Brander and Short, 2001; MacMahan et al., 2005). These results suggest the mean velocities are low with only maxima reaching $O(>1$ m/s). Past suggestions that mean rip speeds are $O(1$ m/s) may be similar to visual observations of waves corresponding to the average of the highest one-third waves, whereby only larger events are noticed and the lower events are ignored.

Rip currents have been observed to pulsate on wave group temporal scales (Shepard and Inman, 1950; Sonu, 1972; Brander and Short, 2001; MacMahan et al., 2004a). Infragravity rip current pulsations increase the instantaneous rip current maximum flow to over 1 m/s over periods of 25–250 s. In addition, stochastically varying wave groups can increase the rip velocity (Callaghan et al., 2004; MacMahan et al., 2004b; Reniers et al., 2005—this issue).

To provide a framework for discussion, the rip current flow is partitioned by frequency bands,

$$U_{rip} = U_{ig} + U_{VLF} + U_{mean} + U_{tide}, \quad (5)$$

where U_{ig} is the contribution within the infragravity band, 0.004–0.04 Hz (25–250 s), U_{VLF} is the contribution within 0.0005–0.004 Hz (4–30 min), U_{mean} is the mean based on the rip current system and wave conditions, and U_{tide} is the modulation associated with slow variations in the water level.

3.1. Low frequency pulsations (infragravity)

Rip current pulsations are generally associated with wave groups at the infragravity band (0.004–0.04Hz) (Shepard et al., 1941; Shepard and Inman, 1950; Sonu, 1972; Aagaard et al., 1997; Brander and Short, 2001; MacMahan et al., 2004a). The original hypothesis was that the mass transport and wave set-up (hydraulic head) produced by the higher waves within wave groups ponds significant amounts of water within the surf zone. During the subsequent minima in the short-wave groups, the ponded water returns outside the surf zone through the rip channels, which are hydraulically more efficient (Munk, 1949a,b; Shepard and Inman, 1950). Therefore, the flow is pumped over the bar with the incoming short-wave groups and primarily returns through the rip channel.

A second hypothesis is that the rip current pulsations are due to infragravity cross-shore standing waves (surfbeat by Sonu, 1972). This was confirmed at RIPEX (MacMahan et al., 2004a; Reniers et al., 2005—this issue), where the infragravity contribution ($\sqrt{u_{rms,ig}^2 + v_{rms,ig}^2}$) was computed for 10 days, when there was minimal alongshore profile change (Fig. 7). The relatively large alongshore differences in the $U_{rms,ig}$ are statistically significant with the 95% confidence interval. The $U_{rms,ig}$ variations are associated with alongshore differences in bathymetric elevations, owing to the infragravity velocities inverse dependence on depth given by,

$$U_{rms,ig} = \eta_{rms,ig}\sqrt{\frac{g}{h}}, \quad (6)$$

where $\eta_{rms,ig}$ is infragravity sea surface elevation and h is the water depth, which are consistent with previous observations of infragravity motions (Suhayda, 1974; Guza and Thornton, 1985; amongst others). Thus, the magnitude of the $U_{rms,ig}$ is smaller within the rip channel, where the depth is greater. Similar results were found during NCEX (Nearshore Canyon EXperiment) (MacMahan et al., submitted for publication).

3.2. Very low frequency pulsations

Smith and Largier (1995) observed 15-min oscillations/pulsations of a rip current jet outside of the breaker region. Haller and Dalrymple (2001), using monochromatic waves within the laboratory, observed that the rip current jet was unstable owing to the current shear, and referred to these motions as rip current instabilities. Brander and Short (2001) re-examined their original data set and found energetic velocity variance for frequencies less than 0.004 Hz. MacMahan et al. (2004b) found energetic motions for frequencies less than 0.004 Hz during RIPEX, referred to as very low frequency motions (VLFs). The VLFs within frequency-wave number spectra are outside the gravity restoring region, indicating these are horizontal vortices. The VLF energy occurred at alongshore wave number corresponding to alongshore spacing of rip channels, suggesting that they were coupled to the underlying morphology. The VLF intensity increased with increasing wave energy. During RIPEX, energetic VLFs were observed throughout the experiment.

Callaghan et al. (2004) found that very slow modulations in wave energy and rip current velocity were qualitatively correlated over a transverse barred beach displaying increased rip current velocities with increasing wave energy (Fig. 8). In contrast, the wave energy modulation for the longer RIPEX

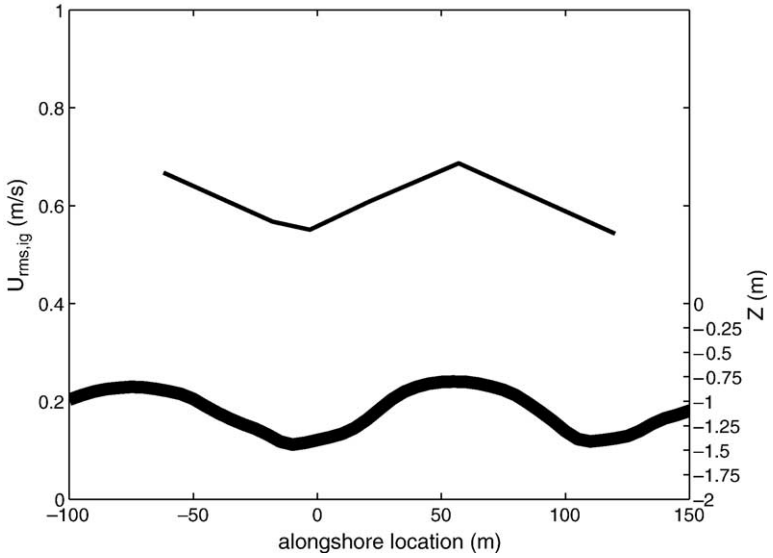

Fig. 7. $U_{rms,ig}$ for 10 days within the alongshore array during RIPEX (from MacMahan et al., 2004a). The 95% confidence interval is represented by the thickness of the $U_{rms,ig}$ curve. The corresponding bed level along the array at approximately mid-surf zone is shown as a thick curve (bed level labelled on the right-hand side). Reproduced from MacMahan et al. (2004a) with permission from the American Geophysical Union.

data set did not have the same high correlation. Also, for an alongshore uniform beach, model predicted wave height modulation and cross-shore currents do not have significant correlation (Reniers et al., 2004), similar to the results by Tang and Dalrymple (1989).

3.3. Tides

Rip currents have long been observed to vary with the tidal elevation, and rip tide is a common misnomer of rip currents. Rip currents are little affected by tidal currents. Rip currents are tidally modulated, such that decreases in tidal elevation increase rip current flows to a relative maximum (Sonu, 1972; Aagaard et al., 1997; Brander, 1999; Brander and Short, 2001; MacMahan et al., 2005), and the presence and danger of rip currents are often linked to lower tidal elevations (Shepard et al., 1941; McKenzie, 1958; Short and Hogan, 1994; Luschine, 1991; Lascody, 1998; Engle et al., 2002). Hourly mean velocity magnitudes were computed for adjacent rip currents during RIPEX. The rip current velocities have a strong tidal modulation, with increasing speeds occurring with decreasing tidal elevation (Fig. 9), consistent

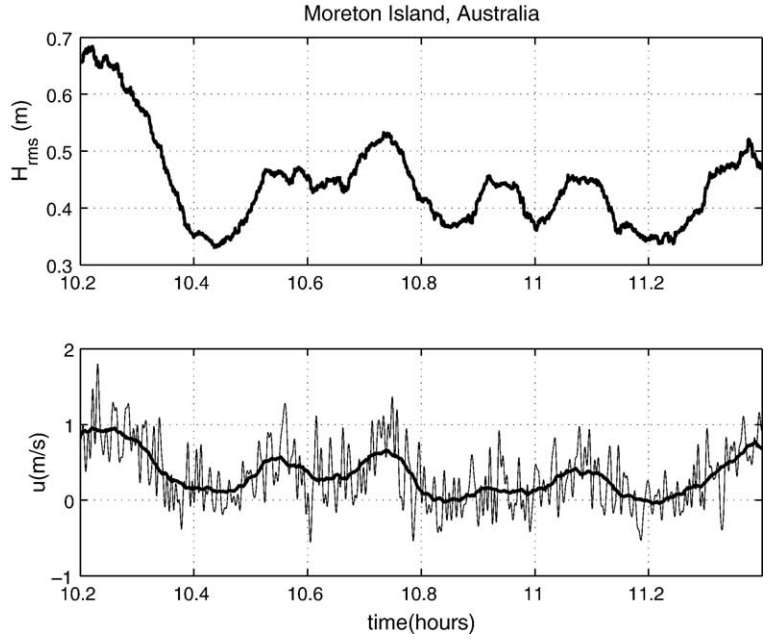

Fig. 8. (Top) low-pass filtered (5-min running mean average) H_{rms} and (bottom) 5-min low-pass filtered and 25–250 s band-passed filtered cross-shore (u) velocity within a rip channel at Moreton Island, Australia. Positive values are offshore.

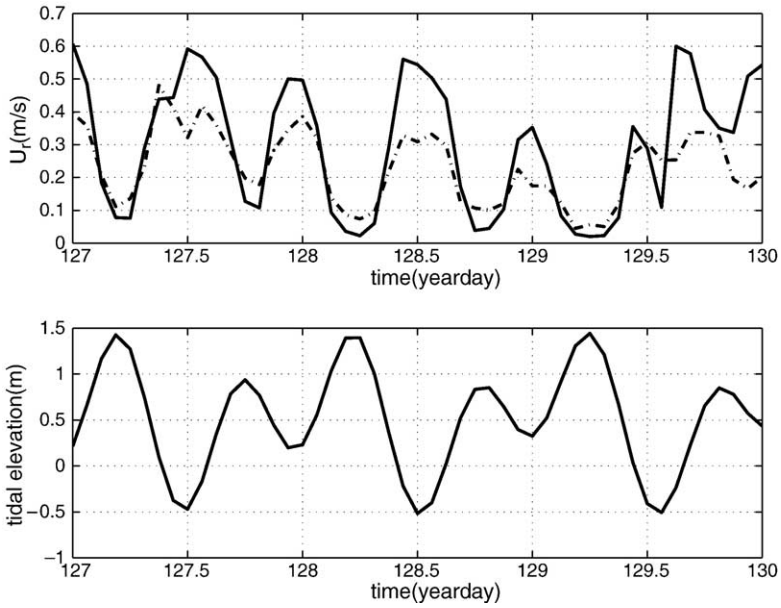

Fig. 9. (Top) for RIPEX, the tidal modulation of rip currents speeds (90-min averages) was recorded within adjacent rip channels (at depths of 1 m) for several days, when the wave conditions were relatively constant. (Bottom) concurrent tidal elevation relative to MSL. Reproduced from MacMahan et al. (submitted for publication) with permission from the Elsevier.

with previous field observations. At high tides, the rip current is non-existent (Sonu, 1972; Aagaard et al., 1997; Brander, 1999; Brander and Short, 2001; MacMahan et al., 2005). During times of spring tides, the threat of rip currents to beach-goers and the potential influence of the rip currents transporting sediments increases until the water depth over the shoal becomes too shallow or dry.

In summary, the rip current flow consists of various temporal contributions, all of which have their own forcing mechanism. The combination results in significant flow speeds that have the potential for transporting sediment and catching beach-goers off-guard. For RIPEX, the contributions were

$$\begin{aligned} U_{\mathrm{rip}}(1-2\ \mathrm{m/s}) = {} & U_{\mathrm{ig}}(0.65\ \mathrm{m/s}) + U_{\mathrm{VLF}}(0.50\ m/s) \\ & + U_{\mathrm{mean}}(0.35\ \mathrm{m/s}) \\ & + U_{\mathrm{tide}}(0.30\ \mathrm{m/s}), \end{aligned} \tag{7}$$

which at times produced fast rip currents.

4. Rip scaling

4.1. Rip current dynamic scaling

As stated above, the mean velocity of a rip currents varies for different beaches, wave forcing, and tidal elevation.

The Froude number (Fr) provides a dimensionless measure of the rip current flow, which is defined as

$$Fr = U_{\mathrm{r}}/\sqrt{gh}, \tag{8}$$

where U_{r} is the velocity within the rip channel and $\sqrt{gh}$ is equal to the wave group velocity or phase speed in shallow water (Dronen et al., 2002; Haller et al., 2002; MacMahan et al., 2005). Laboratory and field (RIPEX) data indicate that rip current velocity increases with increasing wave height and decreasing water depth. Thus, the dimensionless variable H/h (wave height/water depth) is used to parameterize forcing intensity. During laboratory experiments the parameterized water depth is taken as the depth at the top of the bar crest (Dronen et al., 2002; Haller et al., 2002). MacMahan et al. (2005) for consistency did the same for field measurements (Fig. 10). The overall trend suggests that rip velocities increase with increasing wave height and decreasing water elevations, which is consistent with previous observations (Shepard and Inman, 1950; Sonu, 1972; Aagaard et al., 1997; Brander, 1999; Brander and Short, 2001; MacMahan et al., 2005, amongst others).

The relative depth of the rip channel $h_{\text{rip-channel}}/h_{\text{bar}}$ is in general deeper in the laboratory (2.5–5) compared with the field (1.2–2.7, Table 3). The deeper channels have the effect of increasing the flow efficiency (Nielsen et al., 2001) and wave–current interaction (discussed in *Rip Current Kinematic Scaling*). It is hypothesized that there is an equilibrium depth for a rip channel with a sandy bottom based on the local maximum scour depth. However, there is not enough field data available to determine this.

The alongshore perturbation in the bathymetry can vary from a strong signature, as observed during RIPEX with deeply incised tidal terraces at a alongshore channel slope of 1:20, to a weak signal, observed during NCEX, with a slight depression on a near-planar beach with a 1:300 slope (Fig. 11). Both beaches produced morphologically-controlled rip currents. The NCEX bathymetry suggests that subtle bathymetric perturbations can induce significant three-dimensional flows.

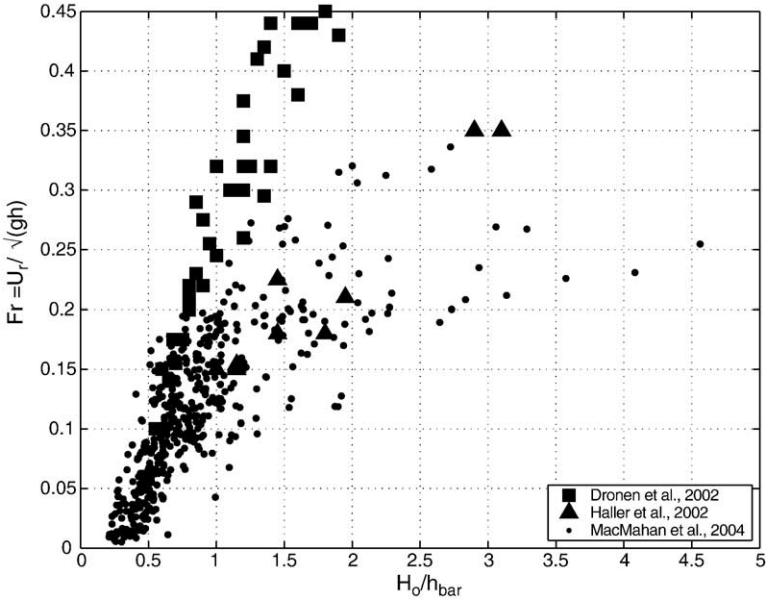

Fig. 10. Dimensionless return flow, U_r, as function of H_o/h_{bar} for Dronen et al. (2002), Haller et al. (2002) and MacMahan et al. (submitted for publication).

4.2. Rip current kinematic scaling

Wave–current interactions affect the wave height within the rip channel, where an increasing current leads to increasing wave heights owing to wave steepening, until wave breaking occurs. We define the following classification of rip currents, low, intermediate, and high energy systems, which are related to wave–current interaction and inversely related to the wave energy within the rip channel. All available data are combined to em assess the importance of wave–current interaction (Fig. 12). *Fr* represents the importance of wave–current interaction, which is useful in describing the hydrodynamics of the rip current system (Haller and Ozkan-Haller, 2003). Low energy rip currents have minimal wave–current interaction. An example of this is NCEX, where the rip morphology is subtle and the wave energy was relatively low (MacMahan et al., submitted for publication). Observations most commonly fall within the class of intermediate energy rip currents that have moderate wave–current interaction. Increasing the wave height (without breaking) within the rip channel creates a negative feedback on the system, because the radiation stress gradients develop a counter torque that oppose the pressure gradients (Oh and Dean, 1996; Haller et al., 2002; Haas et al., 2003). Yu and Slinn (2003) also suggest a negative feedback for wave breaking in the rip channel based on numerical models. When the current becomes fast enough, wave breaking occurs within the rip channel and the opposing radiation stress is reduced and a positive feedback mechanism occurs, increasing the rip

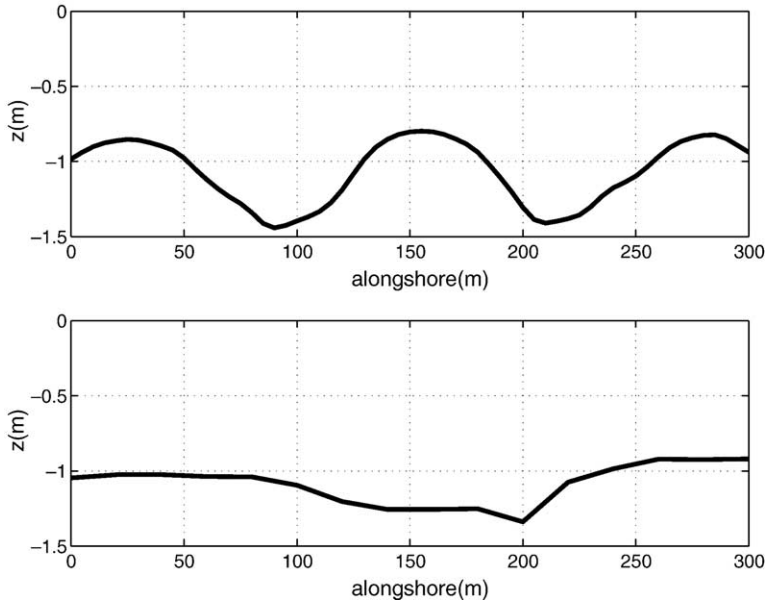

Fig. 11. Alongshore bathymetric profile for RIPEX (top) and NCEX (bottom) relative to MSL in the mid-surf zone.

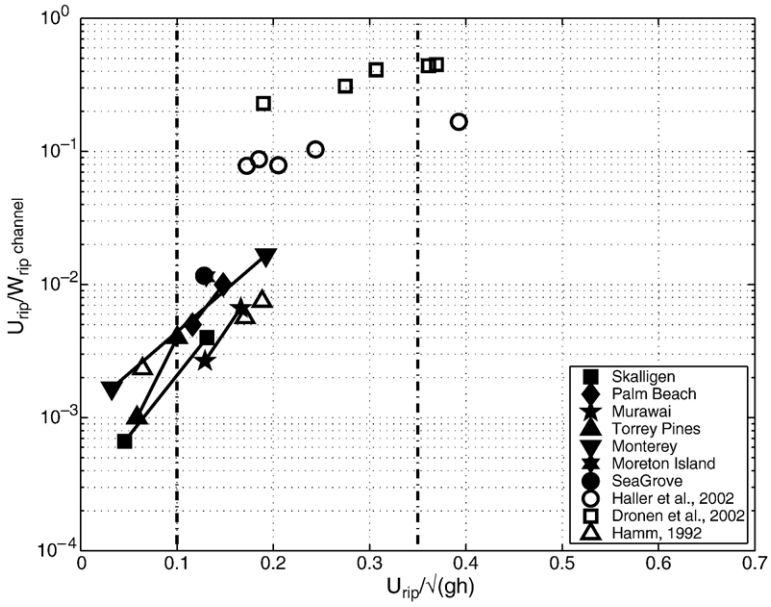

Fig. 12. Strength of rip current measured by Froude Number, $Fr = U_{rip}/\sqrt{gh}$ versus shear of rip current $U_{rip}/W_{rip\text{-}channel}$. Open symbols are laboratory experiments. Lines connecting symbols represent the relative minimum and maximum values during the experiment. Bold dashed vertical lines divide the data into low, intermediate and high energy rip current regimes.

current flow. Therefore, the larger the wave height in the rip channel, the larger the opposing force (negative feedback). Haller and Dalrymple (2001) observed breaking for all of their cases, but the wave heights were generally larger within the rip channel and broke closer to shore, except for their Case D, which had intense wave breaking. High energy rip currents have significant wave–current interaction inducing significant wave dissipation. The maximum mean Fr is 0.4 (Fig. 12), which was observed to have a positive feedback (see Haller et al., 2002, case D). The opposing radiation stress gradients are reduced and the rip current velocity increased (Haller et al., 2002). This case is hypothesized to represent a mega-rip. For each of these three classes, the forcing and feedback varies.

There is a division between the field and laboratory measurements around $U_{rip}/\sqrt{gh} = 0.17$, with field measurements occurring for smaller Froude numbers. All Froude numbers are much less than one. We arbitrarily set the low energy cut-off at 0.1 and the high energy limit at 0.35 (Fig. 12). The importance of wave–current interaction within the laboratory has greater significance than documented in field measurements, thus far. The lines represent the minimum and maximum values obtained for the particular experiments, which suggests that wave–current interaction is important under different wave conditions and tidal elevations. As discussed above, rip currents pulsate, which will increase the relative importance of the wave–current interaction and the feedback mechanism. Haas et al. (2003) discussed the temporal variability and the feedback mechanism, which may be responsible for pulsating a rip current.

4.3. Rip current shear

The rip current shear determines the potential for the onset of rip current instabilities (Haller and Dalrymple, 2001), and is approximated by the dimensional parameter $U_{rip}/W_{rip\text{-}channel}$, where $W_{rip\text{-}channel}$ is the width of the rip channel. Shear in laboratory experiments is generally one order of magnitude larger than observed in the field (Fig. 12). Interestingly, shear is also larger for smaller rip current systems, which form closer to shore, referred to as mini-rips (Short, 1999). Haller and Dalrymple (2001) observed that the rip current meandered within the rip channel. Thus the shear may be larger for the laboratory measurements, but there are no detailed measurements across a rip channel to evaluate this in the field. It is hypothesized that the shear would also be important for mega-rips, yet there are no measurements to confirm this. Episodic instability plumes are often observed outside the breaker region (Smith and Largier, 1995). It is unclear when these visual markers appear and how they are related to the instabilities (see *Vertical structure* for more discussion).

4.4. Rip current morphology

Wright and Short (1984) use the non-dimensional fall velocity parameter, $\Omega = H/T/w_s$, to determine beach states, and the available data are examined as to how Ω is related to Fr (Fig. 13). The intermediate beach states ($\Omega = 2–5$) are characterized by rip current morphology, which is where most of the data occur. As Ω decreases, the energy of the rip current system increases. This metric provides a qualitative assessment of the system, but the mean properties of the system are often not representative of the conditions that are responsible for the development of rip channels.

Attempts have been made to relate the scales of rip current morphology to the local wave climate, shoreline orientation, sediment size, and tidal conditions (Short and Brander, 1999). Rip locations based on daily visual observations over a 19 month period were reported by Short (1985) and later re-

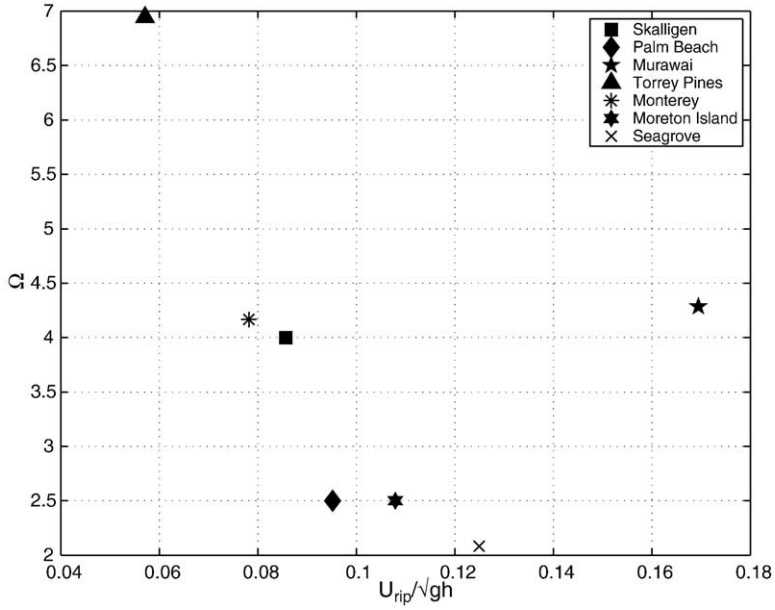

Fig. 13. Non-dimensional scaling for $U_{\mathrm{rip}}/\sqrt{gh}$ versus Ω for mean experimental values.

examined by Huntley and Short (1992). Additionally, Short and Brander (1999) attempted to correlate rip current spacing with average wave properties and sedimentary characteristics. All these analysis produced surprisingly poor correlation between rip spacing and wave height, surf zone width and wave period. Huntley and Short (1992) note the poor correlations may be due in part to the uncertainties in the visual observations, particularly estimates of surf zone width. The rip channel spacing varies considerably (Ranasinghe et al., 2002; MacMahan, 2003). Holman et al. (in press) analyzed four years of rip current spacing at Palm Beach, Australia and measured a coefficient of variation of 0.39, defined as the standard deviation divided by the mean spacing. Reniers et al. (2004) predict a coefficient of variation of 0.36 over the nominal range of mean directional spread of 5° to 22° (see Fig. 4).

5. Rip current flow structure

5.1. Vertical structure

Measurements of the vertical structure of rip currents in the field are limited. Sonu (1972) obtained some information of the vertical structure within wading depths, but a full detailed description of the observation is lacking. Brander and Short (2001) used three ducted impellor current meters over the vertical to measure velocity profiles. During RIPEX, the vertical structure of the flow field was measured on the transverse bar with a vertical array of eight bidirectional em current meters (Fig. 14). The flow was mostly either shoreward or alongshore, and no return flow (undertow) occurred. The measurements found little variation over the vertical.

Within the rip current outside of the surf zone, stronger shear between the surface layer and flow beneath is indicated by available measurements. Haas and Svendsen (2002) found vertical velocity profiles were essentially uniform below the wave trough within the surf zone along the axis of a rip channel. Kennedy and Thomas (2004) used surface drifters in the same laboratory setting as Haas and Svendsen (2002). Their measurements suggest significant onshore flow contribution at the surface due to Stokes drift and the roller, with a strong seaward flow occurring below the trough. This results in significant shear over the vertical, in particular near the surface. Vertical velocity profiles were measured with an aquadopp deployed in the rip channel shoreward of the breaking region during RIPEX. The aquadopp has the capability to measure the mass flux between the trough and crest.

Analysis of the aquadopp measurements indicates that there is significant shear near the surface with the offshore flowing rip current retarded near the surface owing to onshore mass transport of waves (Fig. 15). In the absence of waves, the velocity profile would uniformly extend to the mean sea level (MSL), $z/h=1$. Within the surf zone and in a Eulerian reference frame, the presence of waves induces an onshore Stokes drift counter to the rip current near the surface, which results in a significant vertical shear in the crest–trough region (Fig. 15) (MacMahan et al., 2005). The normalized Stokes drift, $\frac{E}{\rho C^2 H_{\mathrm{rms}}}0.1$, is comparable to the measured deficit at MSL. The surface flow field is different than the underlying flow field (within the surf zone), supported by drifter observations in the laboratory (Kennedy and Thomas, 2004) and field (Schmidt et al., 2003).

Outside the surf zone, Haas and Svendsen (2002) found the mean velocities were near zero, although instantaneous velocities could be substantial. This is associated with the pulsing and unstable nature of the rip current (Haller and Dalrymple, 2001). Utilizing an average binning method, which captures the presence of the offshore rip current jet, they found that the jet flow is surface dominant seaward of the breaking region. Therefore, the visual markers such as sediment plumes

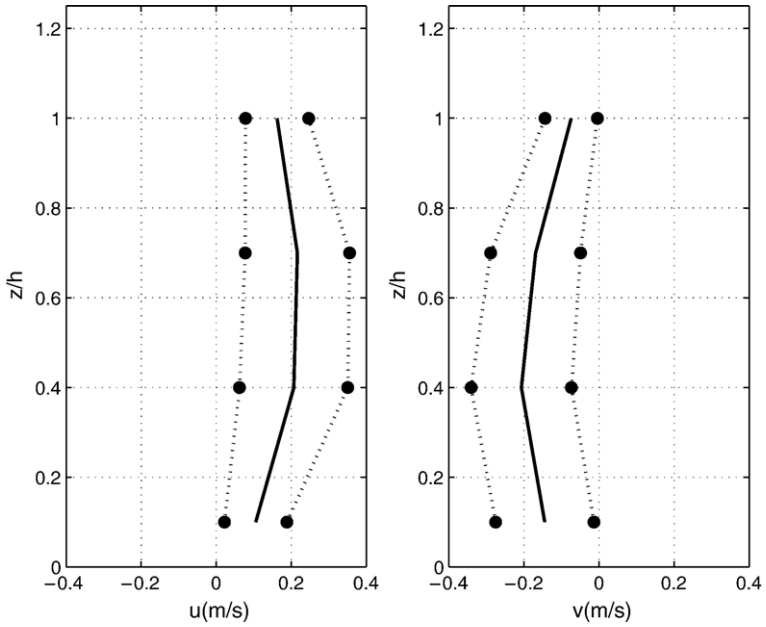

Fig. 14. Averaged (solid) vertical distributions of cross-shore (left) and alongshore (right) velocities on the transverse bar round MSL during RIPEX (MacMahan et al., submitted for publication). Dotted lines represent one standard deviation.

or bubbles associated with rip currents seen outside of the surf zone are surface dominated and their average propagation speed is minimal.

5.2. Cross-shore flow distribution

The description of the cross-shore flow distribution requires velocity measurements in the cross-shore along with wave heights to give a location reference relative to the breaker line. The maximum wave height in the cross-shore is assumed to be the location of the mean breaker location, which defines the width of the surf zone (Thornton and Guza, 1983). The available laboratory measurements are for an incised-channel on a barred beach (Haller et al., 2002; Haller and Ozkan-Haller, 2003) and for an incised-channel on a planar beach (Hamm, 1992). The only field data available are for an incised-channel on a near-planar beach during the field experiment NCEX (MacMahan et al., submitted for publication) (Fig. 16). The surf zone width was approximately 100 m and the rip current maximum is at mid-surf zone (53 m), which coincides with the maximum in the longshore current.

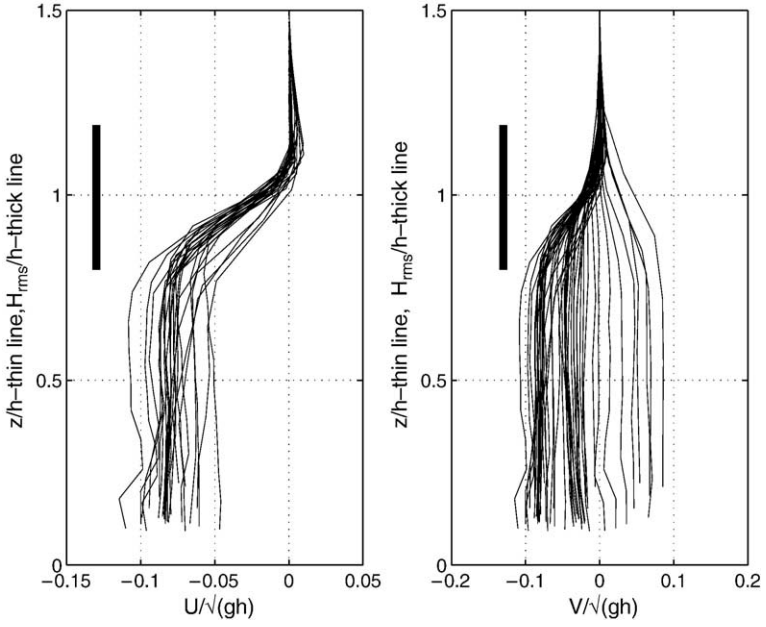

Fig. 15. Vertical distributions of cross-shore (left) and alongshore (right) velocities within the rip current. The mean water level is located at $z/h=1$. H_{rms} is indicated by the bold vertical line, representing the range of values, and indicates that most of the shear is in the crest–trough region Reproduced from MacMahan et al. (submitted for publication) with permission from the Elsevier.

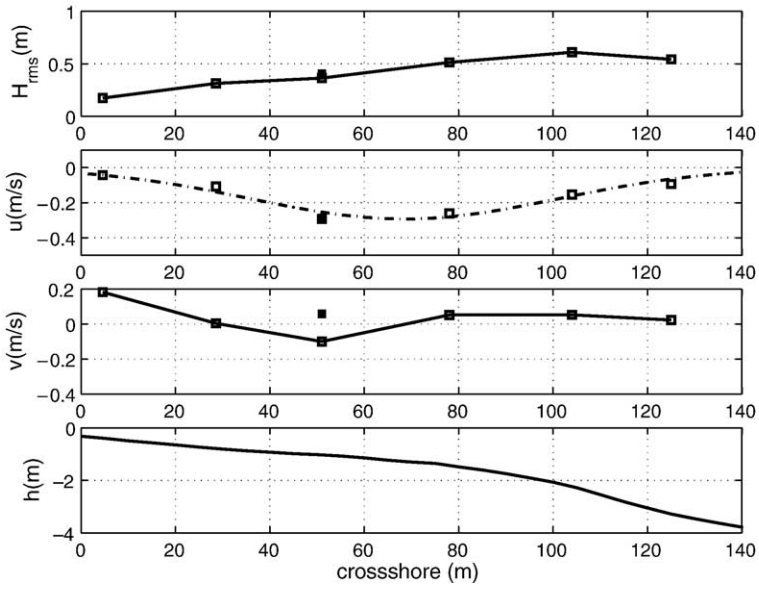

Fig. 16. The cross-shore distribution of H_{rms} (top) and U_{mean}, V_{mean} (middle), and h (bottom) for NCEX. The dash lined represents a Gaussian fit (Haller and Ozkan-Haller, 2003).

The cross-shore location (X) of $U_{max,avg}$ and $H_{max,avg,rms}$ is determined. $X(H_{max,avg,rms})$ represents one surf zone width, therefore $X_{rip}=X(U_{max,avg})/X(H_{max,avg,rms})$ represents the percentage of the surf zone width where the rip current maximum is located. Hamm (1992) presented three cases, small, intermediate, and large waves. Only the intermediate and large wave case, had enough spatial information for accurate determination of X_{rip}, which equaled 1 and 0.66 for the intermediate and large wave cases. For Haller and Ozkan-Haller (2003), X_{rip} ranged from 0.70–0.87. For NCEX, X_{rip} was 0.53. Therefore, the maximum mean rip current velocity occurs within the surfzone.

Theoretically, it would be expected that the maximum rip current velocity in the cross-shore would occur where the forcing is maximum, as found by Haller et al. (2002) in the laboratory. For the NCEX data, the maximum of the rip velocity and longshore current velocity coincide. Longshore current theory predicts the maximum occurs where the radiation stress gradient is maximum. Therefore, it is assumed the maximum for the rip current coincides with the maximum in the gradients in radiation stress. Haller et al. (2002) suggest that the non-linear terms may be important in shifting the maximum current shoreward, which appears to be consistent with the available observations. Alongshore pressure gradients induced by alongshore bathymetric variations can also move the longshore current maximum shoreward (Putrevu et al., 1995, Reniers, 1999). In addition, Reniers and Battjes (1997) and Ruessink et al. (2001) found that the inclusion of the roller in the wave forcing induces a spatial lag that shifts the maximum of the alongshore current shoreward. The importance of the roller's contribution within rip current systems has not been fully explored.

Haller et al. (2002) found that a counter-current existed close to shore within the vicinity of the rip channel (Fig. 6). The counter-current was associated with an adverse pressure gradient owing to the fact that the waves break closer to shore. There is evidence to suggest that this may occur within the field. The shoreward-most current meter during NCEX measured V_{mean} in the opposing direction of the cellular circulation, which may be related to a counter circulation.

6. Summary and conclusions

Earlier qualitative observations have been quantified and theoretically evaluated with more extensive field and laboratory measurements. Rip currents are observed to pulsate at various temporal scales, which have different forcing. The pulsations are composed of infragravity motions, modulations of wave group energy, shear instabilities, and tides. The summation of these flow contributions can lead to strong offshore rip currents that last for several minutes. The time averaged pulsations are minimal outside the surf zone (within the laboratory), yet when the pulsations occur, they are surface dominated. Data from the laboratory and the field suggest that the rip current strength increases with increasing wave energy and decreasing water depths. Rip currents can occur under various bathymetric perturbations, even for beaches with subtle alongshore variations.

The maximum mean current occurs inside the surf zone, where the maximum forcing is present owing to the dissipation of waves. Wave–current interaction may define the energy of a rip current system and feedback mechanisms. Most laboratory data are for high shear (strong rip with relatively narrow channel) compared with field data. The high shear cases may be representative of mega-rips, which are difficult to measure in the field. High shear leads to instability of the rip jet, which is found in laboratory measurements. The importance of shear under rip current pulsations requires further investigations. The onshore flows over the bar feeding the rip current system is found uniform over the vertical. The offshore flowing rip

current, on the other hand, has high shear at the surface owing to the onshore mass transport velocity of the waves retarding the offshore flow.

Most field observations have been for rip currents coupled to the underlying beach morphology. There have been a few observations of non-stationary rip currents, which are often referred to as transient rip currents (Tang and Dalrymple, 1989; Fowler and Dalrymple, 1990; Johnson and Pattiaratchi, 2004), but detailed documentation is still required. Measurements describing the forcing associated with transient rip currents are desired in particular, since these motions may provide the initial perturbation for the development of rip current channels (Reniers et al., 2004).

Attempts to relate rip spacing to measured wave height, period and sediment characteristics have not been successful (Ranasinghe et al., 2002). Models suggest that the rip spacing may not be sensitive to wave height or mean period of the incident waves, but is dependent on the alongshore length scale of the wave group energy and the direction of the incident waves.

Areas with lack of field measurements include 1) the wave–current interaction along the axis of the rip current under higher wave conditions, 2) the vertical structure of the rip current flow within the breaking and offshore region, 3) offshore pulsation extent and vortex shedding, and 4) mega rips.

Acknowledgements

We extend our thanks to Jurjen Battjes, whose basic formulations of wave set-up, radiation stress, wave breaking and turbulence are central to our understanding of surf zone hydrodynamics amongst many other findings. In 2004, a rip current technical workshop was coordinated by NOAA Sea Grant and NOAA National Weather Service to improve coordination between research scientists and forecasters. The rip current science workshop was sponsored by the Sea Grant's Coastal Hazards Theme Team, Sea Grant programs from DE, NC, FL, NJ, SC, and OR, and the National Weather Service. This manuscript was conceptualized from this workshop. This work was jointly funded by the National Science Foundation under contracts OCE-01366882 and DMS-0234521, the Office of Naval Research under contract N0001405WR20150, and the National Ocean Partnership Program NOPP-N0001404WR20125. Additional funding for A.R. from the Dutch National Science Foundation (NWO), under contract DCB.5856 is much appreciated.

References

Aagaard, T., Greenwood, B., Nielsen, J., 1997. Mean currents and sediment transport in a rip channel. Mar. Geol. 140, 24–45.

Arthur, R.S., 1962. A note on the dynamics of rip currents. J. Geophys. Res. 67 (7), 2777–2779.

Battjes, J.A., 1988. Surf-zone dynamics. Annu. Rev. Fluid Mech. 20, 257–293.

Blondeaux, P., 2001. Mechanics of coastal forms. Annu. Rev. Fluid Mech. 33, 339–370.

Bowen, A.J., 1969. Rip currents: 1. Theoretical investigations. J. Geophys. Res. 74, 5467–5478.

Bowen, A.J., Inman, D.L., 1969. Rip currents: 2. Laboratory and field observations. J. Geophys. Res. 74, 5479–5490.

Bowman, D., Arad, D., Rosen, D.S., Kit, E., Golbery, R., Slavicz, A., 1988a. Flow characteristics along the rip current system under low-energy conditions. Mar. Geol. 82, 149–167.

Bowman, D., Rosen, D.S., Kit, E., Arad, D., Slavicz, A., 1988b. Flow characteristics at the rip current neck under low-energy conditions. Mar. Geol. 79, 41–54.

Brander, R.W., 1999. Field observations on the morphodynamic evolution of low wave energy rip current system. Mar. Geol. 157, 199–217.

Brander, R.W., Short, A.D., 2000. Morphodynamics of a large-scale rip current system at Muriwai Beach, New Zealand. Mar. Geol. 165, 27–39.

Brander, R.W., Short, A.D., 2001. Flow kinematics of low-energy rip current systems. J. Coast. Res. 17 (2), 468–481.

Buhler, O., Jacobson, T.E., 2001. Wave-driven currents and vortex dynamics on barred beaches. J. Fluid Mech. 449, 313–339.

Callaghan, D.P., Baldock, T.E., Nielsen, P., Hanes, D.M., Hass, K., MacMahan, J.H., 2004. Pulsing and circulation in a rip current system. Proceedings of the 29th International Conference on Coastal Engineering. Am. Soc. of Civ. Eng., Portugal, pp. 1493–1505.

Chen, Q., Dalrymple, R.A., Kirby, J.T, Kennedy, A.B., Haller, M.C., 1999. Boussinesq modeling of a rip current system. J. Geophys. Res. 104, 20617–20637.

Cooke, D.O., 1970. The occurrence and geologic work of rip currents off southern California. Mar. Geol. 9, 173–186.

Dalrymple, R.A., 1975. A mechanism for rip current generation on an open coast. J. Geophys. Res. 80, 3485–3487.

Dalrymple, R.A., Lozano, C.J., 1978. Wave–current interation models for rip currents. J. Geophys. Res. 83 (C12), 6063–6071.

Dalrymple, R.A., Eubanks, R.A., Birkemeier, W.A., 1977. Wave induced circulation in shallow basins. J. Waterw., Port Coast., Ocean Div., vol. 102. ASCE, pp. 117–135.

Damgaard, J., Dodd, N., Hall, L., Chesher, T., 2002. Morphodynamic modelling of rip channel growth. Coast. Eng. 45, 199–221.

Deigaard, R., Dronen, N., Fredsoe, J., Jensen, J.H., Jorgensen, M.P., 1999. A morphological stability analysis for a long straight barred coast. Coast. Eng. 36, 171195.

Dodd, N., Blondeaux, P., Calvete, D., De Swart, H.E., Falques, A., Hulscher, S.J.M.H., Rozynski, G., Vittori, C., 2003. Understanding coastal morphodynamics using stability methods. J. Coast. Res. 19 (4), 849–865.

Dronen, N., Karunarathna, H., Fredsoe, J., Sumer, B.M., Deigaard, R., 2002. An experimental study of rip channel flow. Coast. Eng. 45 (3–4), 223–238.

Dyhr-Nielsen, M., Sorensen, T., 1970. Some sand transport phenomena on coasts with bars. Proc. of the 12th International Conference on Coastal Engineering. ASCE, New York, pp. 855–866.

Ebersole, B.A., Dalrymple, R.A., 1980. Numerical modelling of nearshore circulation. Paper Presented at International Conference on Coastal Engineering. Am. Soc. of Civil Eng., Sydney.

Engle, J., MacMahan, J., Thieke, R.J., Hanes, D.M., Dean, R.G., 2002. Formulation of a rip current predictive index using rescue data. Florida Shore and Beach Preservation Association National Conference.

Falques, A., Coco, G., Huntley, D.A., 2000. A mechanism for the generation of wave-driven rhythmic patterns in the surf zone. J. Geophys. Res. 105 (C10), 24,071–24,087.

Fowler, R.E., 1991. Wave group forced nearshore circulation: a generation mechanism for migrating rip currents and low frequency motion. Final Report, Research Report #CACR-91-03. Center for Applied Coastal Research, University of Delaware, Newark, Delaware.

Fowler, R.E., Dalrymple, R.A., 1990. Wave group forced nearshore circulation. Proceedings of the 22nd International Conference on Coastal Engineering. Am. Soc. of Civ. Eng., Delft, pp. 729–742.

Guza, R.T., Thornton, E.B., 1985. Observations of surf beat. J. Geophys. Res. 90, 3161–3171.

Haas, K.A., Svendsen, I.A., 2002. Laboratory measurements of the vertical structure of rip currents. J. Geophys. Res., 107.

Haas, K.A., Svendsen, I.A., Haller, M.C., Zhao, G., 2003. Quasi-three-dimensional modeling of rip current system. J. Geophys. Res., 108.

Haller, M.C., Dalrymple, R.A., 2001. Rip current instabilities. J. Fluid Mech. 433, 161–192.
Haller, M.C., Ozkan-Haller, T., 2003. Wave breaking and rip current circulation. Paper Presented at International Conference on Coastal Engineering. Am. Soc. of Civil Eng., Cardiff, pp. 705–717.
Haller, M.C., Dalrymple, R.A., Svendsen, I.A., 1997. Rip channels and nearshore circulation. Proc. Coast. Dyn., pp. 594–603.
Haller, M.C., Dalrymple, R.A., Svendsen, I.A., 2002. Experimental study of nearshore dynamics on a barred beach with rip channels. J. Geophys. Res. 107 (14), 1–21.
Hamm, L., 1992. Directional nearshore wave propagation over a rip channel: an experiment. Paper Presented at International Conference on Coastal Engineering. Am. Soc. of Civil Eng., Venice.
Holman, R.A., 2000. Pattern formation in the nearshore. In: Seminara, G., Blondeaux, P. (Eds.), River, Coastal and Estuarine Morphodynamics. Springler-Verlag, New York, pp. 141–162.
Holman, R.A., Bowen, A.J., 1982. Bars, bumps and holes: model for the generation of complex beach topography. J. Geophys. Res. 87 (C1), 457–468.
Holman, R.A., Symonds, G., Thornton, E.B., Ranasinghe, R., in press. Rip spacing and persistence on a pocket beach. Mar. Geol.
Hino, M., 1974. Theory on the formation of rip-current and cuspidal coast. Proceedings of the 14th International Conference on Coastal Engineering. Am. Soc. of Civ. Eng., Copenhagen, pp. 901–919.
Huntley, D.A., Short, A.D., 1992. On the spacing between observed rip currents. Coast. Eng. 17 (23), 211–225.
Huntley, D.A., Hendry, M.D., Haines, J., Greenidge, B., 1988. Waves and rip currents on a Caribbean pocket beach, Jamaica. J. Coast. Res. 4, 69–79.
Inman, D.L., Quinn, W.H., 1952. Currents in the surf zone. Proceedings of the 2nd International Conference on Coastal Engineering. Am. Soc. of Civ. Eng., Houston, TX, pp. 24–36.
Johnson, D., Pattiaratchi, C., 2004. Transient rip currents and nearshore circulation on a swell-dominated beach. J. Geophys. Res. 109, C02026. doi:10.1029/2003JC001798.
Kennedy, A.B., Thomas, D., 2004. Drifter measurements in a laboratory rip current. J. Geophys. Res. 109, C08005. doi:10.1029/2003JC001927.
Komar, P.D., 1971. Nearshore cell circulation of the formation of giant cusps. Geol. Soc. Amer. Bull. 82, 2643–2650.
Lascody, R.L., 1998. East central Florida rip current program. National Weather Service In-house Report, p. 10.
Longuet-Higgins, M.S., Stewart, R.W., 1964. Radiation stress in water waves, a physical discussion with applications. Deep-Sea Res. 11 (4), 529–563.
Luschine, J.B., 1991. A study of rip current drownings and weather related factors. Natl. Weather Dig., 13–19.
MacMahan, J., 2003. Phd. Dissertation, University of Florida.
MacMahan, J., Reniers, A.J.H.M., Thornton, E.B., Stanton, T., 2004. Infragravity rip current pulsations. J. Geophys. Res. 109, C01033. doi:10.1029/2003JC002068.
MacMahan, J.H., Reniers, A.J.H.M., Thornton, E.B., Stanton, T.P., 2004. Surf zone eddies coupled with rip current morphology. J. Geophys. Res. 109, C07004. doi:10.1029/2003JC002083.
MacMahan, J.H., Reniers, A.J.H.M., Thornton, E.B., Stanton, T.P., Symonds, G., submitted for publication. Kinematics of low-energy rip currents. J. Geophys. Res.
MacMahan, J., Thornton, E.B., Stanton, T.P., Reniers, A.J.H.M., 2005. RIPEX—rip currents on a shore-connected shoal beach. Mar. Geol. 218, 113–134.
McKenzie, P., 1958. Rip-current systems. J. Geol. 66, 103–113.
Mei, C.C., Liu, P.L.-F., 1977. Effects of topography on the circulation in and near the surf zone-linear theory. J. Estuar. Coast. Mar. Sci. 5, 25–37.
Munk, W.H., 1949a. Surf beats. Trans. Am. Geophys. Union 30, 849–854.
Munk, W.H., 1949b. The solitary wave theory and application to surf problems. Ann. N. Y. Acad. Sci. 51 (3), 376–424.
Nielsen, P., Brander, R., Hughes, M.G., 2001. Rip currents: observations of hydraulic gradients, friction factors and wave pump efficiency. Proceedings of 2001 Coastal Dynamics, Am. Soc. Civ. Eng., pp. 483–492.
Noda, E.K., 1974. Wave induced nearshore circulation. J. Geophys. Res. 79, 4097–4106.
Oh, T.M., Dean, R.G., 1996. Three-dimensional hydrodynamics on a barred beach. Proceedings of the 25th International Conference on Coastal Engineering, Am. Soc. Civ. Eng., pp. 3680–3693.
Peregrine, D.H., 1998. Surf zone currents. Theor. Comput. Fluid Dyn. 10, 295–309.
Phillips, O.M., 1977. The Dynamics of the Upper Ocean, 2nd ed. Cambridge Univ. Press, New York. 336 pp.
Putrevu, U.J., Oltman-Shay, J., Svendsen, I.A., 1995. Effect of alongshore non-uniformities on longshore current predictions. J. Geophys. Res. 100, 16119–16130.
Ranasinghe, R., Symonds, G., Black, K., Holman, R., 2002. Processes governing rip spacing persistence, and strength in swell dominated, microtidal environment, Proceedings of the 27th International Conference on Coastal Engineering, Am. Soc. Civ. Eng., pp. 3680–3693. 493–499.
Reniers, A.J.H.M., Longshore current dynamics, Ph.D. thesis, Delft Univ. of Technol., Delft, Netherlands, 1999.
Reniers, A.J.H.M., Battjes, J.A., 1997. A laboratory study of longshore currents over barred and non-barred beaches. Coast. Eng. 30, 1–22.
Reniers, A.J.H.M, Roelvink, J.A., Thornton, E.B., 2004. Morphodynamic modeling of an embayed beach under wave group forcing. J. Geophys. Res. 109, C01030. doi:10.1029/2002JC001586.
Reniers, A.J.H.M, MacMahan, J., Thornton, E.B., Stanton, T., 2005—this issue. Modeling infragravity motions on a rip-channel beach. Coast. Eng. doi:10.1016/j.coastaleng.2005.10.010.
Ruessink, B.G., Miles, J.R., Feddersen, F., Guza, R.T., Elgar, S., 2001. Modeling the alongshore current on barred beaches. J. Geophys. Res. 106, 22451–22463.
Ryrie, S.C., 1983. Longshore motion due to an obliquely incident wave group. J. Fluid Mech. 137, 273–284.
Sallenger, A.H., Holman, R.A., 1987. Infragravity waves over a natural barred profile. J. Geophys. Res. 92 (C9), 9531–9540.
Sasaki, T., Horikawa, T., 1975. Nearshore current system on a gently sloping bottom. Coast. Eng. Jpn. 18, 123–142.
Sasaki, T., Horikawa, K., 1978. Observation of nearshore current and edge waves. Coastal Engineering 1978. Am. Soc. of Civ. Eng., Reston, Va, pp. 791–809.
Schmidt, W., Woodward, B., Millikan, K., Guza, R., Raubenheimer, B., Elgar, S., 2003. A GPS-tracked surf zone drifter. J. Atmos. Ocean. Technol. 20 (7), 1069–1075.
Schmidt, W. Guza, R. Slinn, D.N., in press. Surfzone currents over irregular bathymetry: drifter observations and numerical simulations. J. Atmos. Ocean. Technol.
Shepard, F.P., 1936. Undertow, rip tide, or “rip current”. Science 84.
Shepard, F.P., Inman, D.L., 1950. Nearshore water circulation related to bottom topography and refraction. Trans. Am. Geophys. Union 31, 196–212.
Shepard, F.P., Emery, K.O., La Fond, E.C., 1941. Rip currents: a process of geological importance. J. Geol. 49, 337–369.
Short, A.D., 1985. Rip current type, spacing and persistence, Narrabeen Beach, Australia. Mar. Geol. 65, 47–71.
Short, A.D., 1999. Handbook of Beach and Shoreface Morphodynamics. John Willey and Sons, p. 379.
Short, A.D., Brander, R., 1999. Regional variations in rip density. J. Coast. Res. 15 (3), 813–822.
Short, A.D., Hogan, C.L., 1994. Rip currents and beach hazards, their impact on public safety and implications for coastal management. In: Finkl, C.W. (Ed.), Coastal Hazards, Journal of Coastal Research, Special Issue, vol. 12, pp. 197–209.
Smith, J.A., Largier, J.L., 1995. Observations of nearshore circulation: rip currents. J. Geophys. Res. 100, 10967–10975.
Sonu, C.J., 1972. Field observations of nearshore circulation and meandering currents. J. Geophys. Res. 77, 3232–3247.
Sorensen, O.R., Schaffer, H.A., Madsen, P.A., 1998. Surf zone dynamics simulated by a Boussinesq type model: III. Wave induced horizontal nearshore circulations. Coast. Eng. 33 (2–3), 155–176.

Suhayda, J.N., 1974. Standing waves on beaches. J. Geophys. Res. 79, 3065–3071.
Svendsen, I.A., Haas, K.A., Zhao, Q., 2000. Analysis of rip current systems. In: Edge, B.L. (Ed.), Coastal Engineering, Proceedings of 27th International Conference. Am. Soc. Civ. Eng., New York, pp. 1127–1140.
Symonds, G., Ranasinghe, R., 2000. On the formation of rip currents on a plane beach. Proc. 27th Int. Conf. Coastal Eng.. ASCE, Sydney, pp. 468–481.
Tang, E.C.-S., Dalrymple, R.A., 1989. Nearshore circulation: rip currents and wave groups, Nearshore Sediment Transport, R.J. Seymour., Plenum Press.
Thornton, E.B., Guza, R.T., 1983. Transformation of wave height distribution. J. Geophys. Res. 88, 5925–5938.
Vagle, S., Farmer, D.M., Deane, G.B., 2001. Bubble transport in rip currents. J. Geophy. Res. 106, 11677–11689.
Van Enckevort, I.M.J., Ruessink, B.G., Coco, G., Suzuki, K., Turner, I.L., Plant, N.G., Holman, R.A., 2004. Observations of nearshore crescentic sandbars. J. Geophys. Res. 109, C06028. doi:10.1029/2003JC002214.
Wright, L.D., Short, A.D., 1984. Morphodynamic variability of surf zones and beaches: a synthesis. Mar. Geol. 70, 251–285.
Wu, C.-S., Liu, P., 1985. Finite element modeling of nearshore currents. J. Waterways Port Coastal Ocean Div.. ASCE, pp. 417–432.
Yu, J., Slinn, D.N., 2003. Effects of wave–current interaction on rip currents. J. Geophys. Res. 108, 3088. doi:10.1029/2001JC001105.